Chapter 9

Stimulated Raman Scattering for All Optical Switches

Ariel Flores-Rosas, Evgeny A. Kuzin,
Orlando Díaz-Hernández,
Gerardo J. Escalera-Santos, Roberto Arceo-Reyes,
Baldemar Ibarra-Escamilla and Víctor I. Ruiz-Pérez

Additional information is available at the end of the chapter

http://dx.doi.org/10.5772/66320

Abstract

We theoretically and experimentally investigate an all optical switch based on stimulated Raman scattering in optical fibers. The experimental setup consists of a Raman circuit of two stages connected in series through a bandpass filter. In the first stage, we have a saturated amplifier, in this stage the pump pulses are saturated when pump and signal are launched to the input or the pump pulses remain without saturation when pump only is launched at the input. The second stage works as the Raman amplifier; for this stage amplification is directly dependent on the pump power entering from the first stage. For the case when pump pulse only is launched at the input pass to the second stage without saturation and amplifies the signal entering in the second stage, very intense signal pulses appear at the output of this stage. For the case when both pump and signal pulses are launched to the input, the pump pulse is saturated in the first stage and the filter rejected the amplified signal, so that only low power pump enters the second stage and consequently no signal pulses appear at the output. We show that the contrast can be improved when using fibers with normal and anomalous dispersion connected in series in the first stage. The best contrast (the ratio of energies) obtained was 15 dB at 6 W pump peak power.

Keywords: fiber optics, fiber nonlinearities, optical signal processing, stimulated Raman scattering, optical switch

1. Introduction

All-optical signal processing can be applied in the fields of optical communication and computation for its high speed. As a fundamental and key part for all-optical signal processing,

whose operation relies on nonlinear optical phenomena, has raised great interests in recent years as an alternative to electronic switching in optical communication systems [1, 2]. These devices have a strong potential and can be very useful for a number of applications in diverse areas such as ultrahigh-speed optical telecommunications, wavelength conversion, pulse regeneration, optical monitoring, optical computing, etc. Nonlinear effects will be particularly important in the next generation of optical networks, which will rely on all-optical functions for higher speed and greater capacity. Many principles and devices have been reported; of them a great part is performed by devices based on the Kerr effect in optical fibers, such as the nonlinear optical loop mirror (NOLM) first proposed by Doran and Wood [3], devices based on cross-phase modulation (XPM) proposed by Mamyshev and four-wave mixing (FWM) proposed by Caramella and Stefano [4, 5], logic gates [6], and wavelength conversion [7]. First reports were followed by numerous investigations proving high performance of all-fiber devices. The NOLM was investigated for soliton switch [8], wavelength demultiplexing [9], mode locking [10], etc. Some interferometric devices such as NOLM present an oscillating power transfer function but the ideal characteristic is the step-like function. The power transfer function of the FWM-based devices approaches the step-like function; nevertheless, for an only stage scheme, a flat response is obtained only at spaces, whereas at marks an oscillating dependence was measured [11]. A flat response was shown in double stage scheme at both spaces and marks [12].

Recently, there has been a lot of interest in stimulated Raman scattering (SRS) and is considered one of the most important nonlinear effects in optical fibers. SRS is one of the oldest and most well-studied optical phenomena and can anticipate great advantages for optical signal processing circuits because of high amplification of the signal and naturally existing possibility for wavelength conversion. In spite of that, SRS has just obtained some attention in the context of Raman amplifiers and only a few works were published on the use of SRS for designing optical signal processing circuits and optical switches. Furthermore, SRS can be hoped to present many advantages due to high amplification of the signal and intrinsical compatibility with communications systems using Raman amplification of signals [13]. The strong dependence of the Raman amplification on pump power that was considered for wavelength conversion with high extinction ratio of the output signal and can be base for the design of Raman circuits [14]. In this work, the output signal pulses at Stokes wavelength are generated as result of the Raman amplification caused by input signal used as the pump. Because of the strong dependence of Raman amplification on pump power, the extinction ratio of the output signal can be much higher than that of the input signal. The exploitation of pump saturation in presence of the signal was shown in [15]. In this work, the pulses at Stokes wavelength are used as input signal, and the pump pulses are considered as an output signal. In the absence of the Stokes pulse (spaces), the pump pulse travel in the fiber without saturation and has high power at the fiber output (marks), whereas in presence of the Stokes signal (marks) the pump pulse is depleted and has a low power at the fiber output (spaces). Disadvantage of this approach is the low extinction ration of the output signal. The most interesting work was suggested by Belotiskii [16] where authors used a two-stage setup. In this work, we consider experimentally, the Raman circuit using the approach suggested in [16] and show that it allows the step-like power transfer function with high differential gain and low input signals.

http://dx.doi.org/10.5772/66320

2. Theoretical analysis

In this section, we present simple numerical calculations to show the basic principles and potential of the approach [17]. **Figure 1** presents the diagram of the Raman circuit, it consists of two stages. In stage 1, the pump pulses are saturated if the signal is at "ON" or passes through stage 1 without saturation if the signal is at "OFF," this means that stage 1 woks as saturated amplifier. The amplification in stage 2 depends on the pump power entering from stage 1; that is, stage 2 works as Raman amplifier. When the pump pulse enters stage 2 without saturation as a result of that the input signal is at "OFF," then this will result in the generation of the high output pulses at the Stokes wavelength, this mean that the output signal is at "ON." For the opposite case when the input signal is at "ON," then the pump pulse is depleted in stage 1, the input signal is at "ONs" and therefore the output signal is at "OFF," so in this way the Raman circuit works as an inverter. For this operation of the Raman circuit one should take into account the following considerations: (a) the pump power has to be high enough to provide strong amplification of the signal and (b) at the same time the pump power has to be lower than the SRS threshold at which strong Stokes pulses and pump depletion appears as a result of the amplification of the initial spontaneous Stokes waves. The wavelength of the continuous wave (CW) seeding laser wave defines the wavelength of the output signal. The walk-off effect between pump and Stokes pulses is inevitable because of the big difference between pump and signal wavelengths. To avoid the degradation of the operation of the Raman circuit because of walk-off effect we propose to use the dispersion management using the special fibers, which they are formed by connecting the fibers in which the signal travels faster than pump with the fibers in which the signal travels slower than pump. We must consider that if we use the fibers with anomalous, the modulation instability (MI) effect can be expected, which will complicate circuit operation drastically.

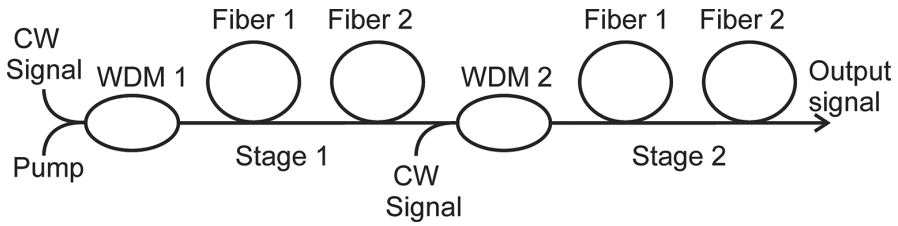

Figure 1. Setup of Raman circuit.

Because of its speed and good results split-step Fourier method (SSFM) is the most commonly used method for numerical analysis of the nonlinear equation of Schrödinger (NLSE), which uses the algorithm's finite Fourier transforms. We use this method to evaluate the operation of the Raman circuit based on the coupled equations for pump A_P, and Stokes A_S, pulses:

$$\frac{\partial A_S(t)}{\partial z} + \left(\frac{1}{V_P} - \frac{1}{V_S}\right)\frac{\partial A_S(t)}{\partial t} + i\frac{\beta_2}{2}\frac{\partial^2 A_S(T,z)}{\partial t^2} = \frac{g}{2}A_S(t)\left|A_P(t)\right|^2 \quad (1)$$

$$\frac{\partial A_P(t)}{\partial z} + i\frac{\beta_2}{2}\frac{\partial^2 A_P(T,z)}{\partial t^2} = -\frac{g}{2}A_P(t)\left|A_P(t)\right|^2 \quad (2)$$

where β_2 is the group velocity dispersion (GVD) parameter considered equal for pump and Stokes wavelengths; g is the Raman gain coefficient equal to 10^{-13} m/W for silica glass at 1550 nm wavelength; V_P and V_S are the group velocity of pump and Stokes pulses, respectively. Here we do not consider the effects connected to the Kerr effect and widening of the pulses due to GVD that is possible if the fiber length is less than the scattering length. The parameters of the fibers used in calculations correspond to the fibers used in experiments. Fiber 1, Corning SMF-LS dispersion shifted fiber with normal dispersion; Fiber 2, SMF-28 fiber with anomalous dispersion; and Fiber 3, OFS True Wave fiber with anomalous dispersion. **Figure 2** shows examples of the pump pulses at the output of Fiber 1 (**Figure 2a**) and at the output of Fiber 2 (**Figure 2b**). Input pulse is shown by the solid line and the output by dashed line.

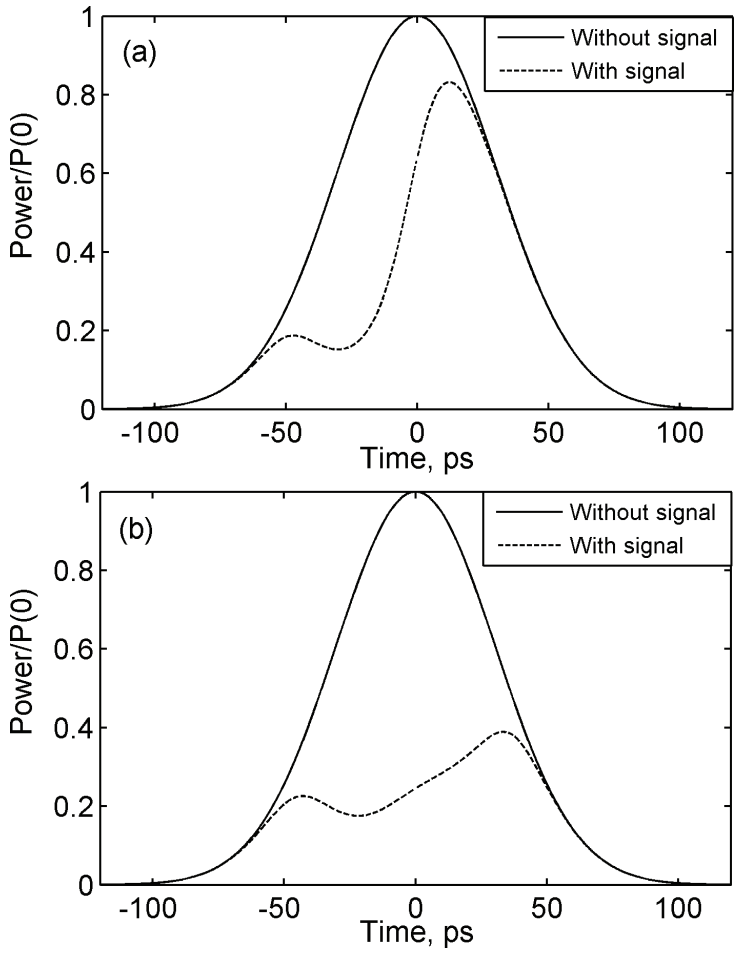

Figure 2. Input (solid line) and output (dashed line) waveforms of the pump at the end of (a) fiber 1 and (b) fiber 2.

http://dx.doi.org/10.5772/66320

The parameters used for calculations were as follow: Fiber 1 SMF-LS with 100 m length, Fiber 2 SMF-28 with 25 m length. The pump pulse presents the Gaussian shape of 100 ps and 25 W of power. The input Stokes pulse has a super Gaussian shape with 300 ps and a peak power of 1 mW and effective area of fibers of 50 μm^2. Fiber 1 has normal dispersion, so Stokes pulse has high speed and the first half of pulse manifests stronger depletion than the second half of pulse. Depletion can be made large when normal dispersion fiber is spliced with a fiber with anomalous dispersion, see **Figure 2(b)**, this happens because in fiber with normal dispersion the signal travels faster than the pump and the fibers with anomalous dispersion the signal travels slower than the pump, therefore pumping depletion becomes stronger in this case [18].

To calculate the depletion of the pump pulse we use as a ratio between the pulse energies at the output and the input. **Figure 3** shows the dependencies of the depletion of the pump on the input Stokes signal peak power. In the figure, the solid line represents the depletion when only the SMF-LS fiber is considered; the fiber length is equals to 100 m (pump power is equals to 30 W). For the dashed line we have 100 m of SMF-LS fiber added with 40 m of SMF-28 fiber (pump power equals to 24 W to have the same total Raman amplification as it was in the first case). Finally, we show the depletion for dotted line and for this case we used 100 m of fiber 1 with low GVD so that walk-off length is much longer than the length of the fiber (pump power was 30 W). It can be seen that the best results obtained are for the fiber with low dispersion; however, in practice it is not easy to fulfill the condition that the walk-off length is larger than the length of the fiber, a special case is when we have low potencies and for this case are required large fiber lengths. However, a simple dispersion management technique using fibers with normal and anomalous dispersion may provide switching with a contrast (the ratio between the energies of the signals at the second stage output) of about 20 dB at input power less than 10^{-3} of pump power [17].

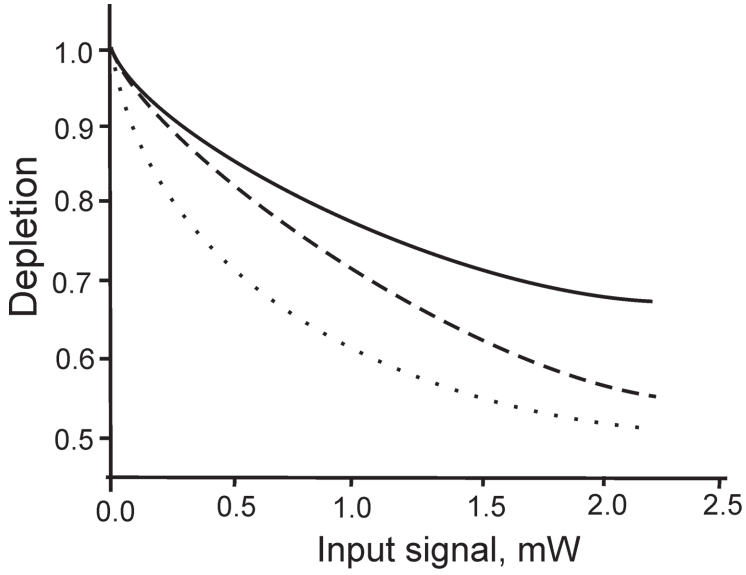

Figure 3. Depletion of the pump at first stage. Solid line is for fiber 1, dashed line is for fiber 1 + fiber 2, and dotted line is for fiber 1 with low dispersion.

We calculate the energy of Stokes pulse of the input in the output circuit depending on the power input Stokes in the first state. The calculations were made with SSFM with $g = 0.6\times10^{-13}$ m/W corresponding to the maximum Raman gain for the pump wavelength 1550 nm, the pulse duration pump of input is 100 ps with a power of 15 W, and the effective area of the fibers is 50 μm^2. Three types of fibers with different GVD were used: fiber 1 D = −6 ps/(nm-km); fiber 2 D = 20 ps/(nm-km); fiber 3 D = −0.01 ps/(nm-km). Fiber 1 corresponds to dispersion shifted fiber, fiber 2 is the SMF-28 fiber, and fiber 3 corresponds to the fiber without walk-off between pulses pump and Stokes. **Figure 4** shows the results for three different configurations of stage 1. Stage 1 is only of fiber 1 with 295 m of length (solid line). Stage 1 is comprised of three fibers connected in series: 150 m of fiber 1, 45 m of fiber 2, and 100 m of fiber 3 (dashed line). Stage 1 is also comprised of 295 m of fiber 3 (the dotted line). For the three cases 350 m of fiber 3 was used for stage 2. The best result is provided by the fiber with low dispersion.

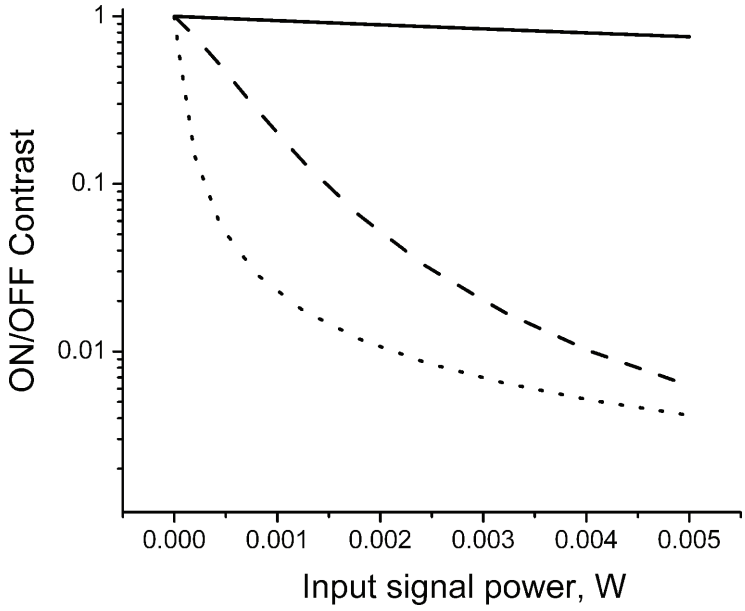

Figure 4. Energy of Stokes pulses at the output of the circuit.

The characteristics of a circuit of two stages depend on the attenuation between them, and two circuits connected in series provide the step-like dependence. The dependence of two circuits for the case when stage 1 is comprised of only fiber 3 and stage 2 is comprised of fiber 3 is shown in **Figure 5(a)**. The dependence for the case when stage 1 is comprised of three fibers connected in series, fiber 1, fiber 2, and fiber 3, and for stage 2 that is comprised of fiber 3 is shown in **Figure 5(b)**. As mentioned earlier, the dependence of two circuits depends on the attenuation between them, and for **Figure 5(a)** and **(b)** the attenuation is different and shows the dependence of the circuits connected in series.

http://dx.doi.org/10.5772/66320

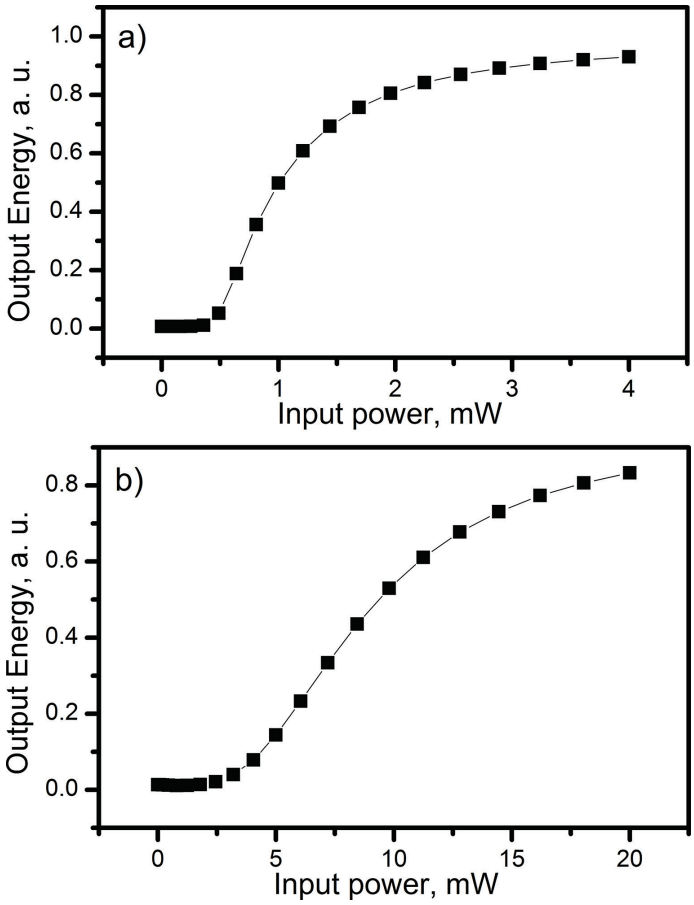

Figure 5. Dependencies of the output Stokes energy on the input power for two circuits connected in series: (a) attenuation is 10 times and (b) attenuation is 3 times.

A strong dependence of the output signal energy on the input signal power allows for improved signal-to-noise ratio of the signal. To show it, we put Gaussian noise to input Stokes. The Gaussian noise added to input Stokes is shown in **Figure 6a)** and the result of the input Stokes with Gaussian noise is shown in **Figure 6(b)**. We can consider two possibilities: one possibility, when input signal is "OFF," Gaussian noise is launched for fiber 1, and two possibility when input signal is "ON," Stokes more Gaussian noise is launched for fiber 1. We applied random noise and the results are show in **Figure 7** for 10 Stokes pulses when input signal is "ON" and "OFF." The parameters of the setup used for calculations were as follows: 100 m of fiber 1, 40 m of fiber 2, and 300 m of fiber 3, input pump power of 24 W, and the power of the input signal of 1 mW. As we can see, the output Stokes pulses are well distinguished [18].

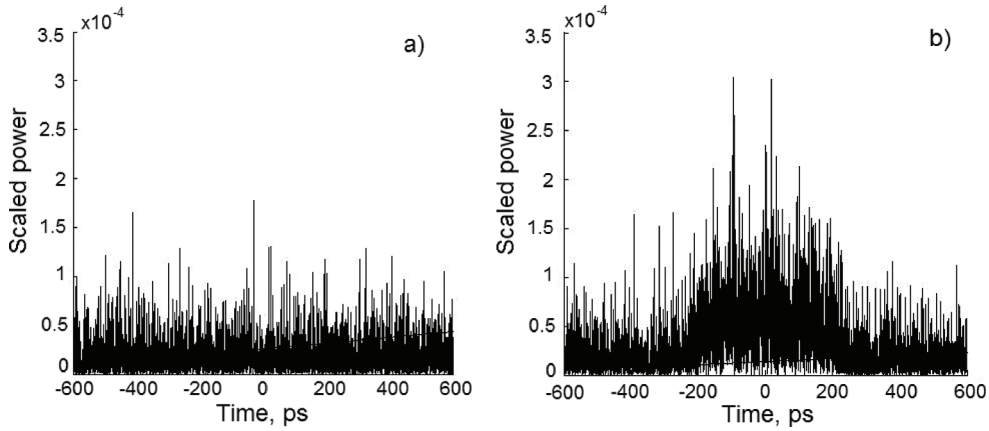

Figure 6. The input signal "off" (a) and the input signal "on" (b) in the presence of random noise.

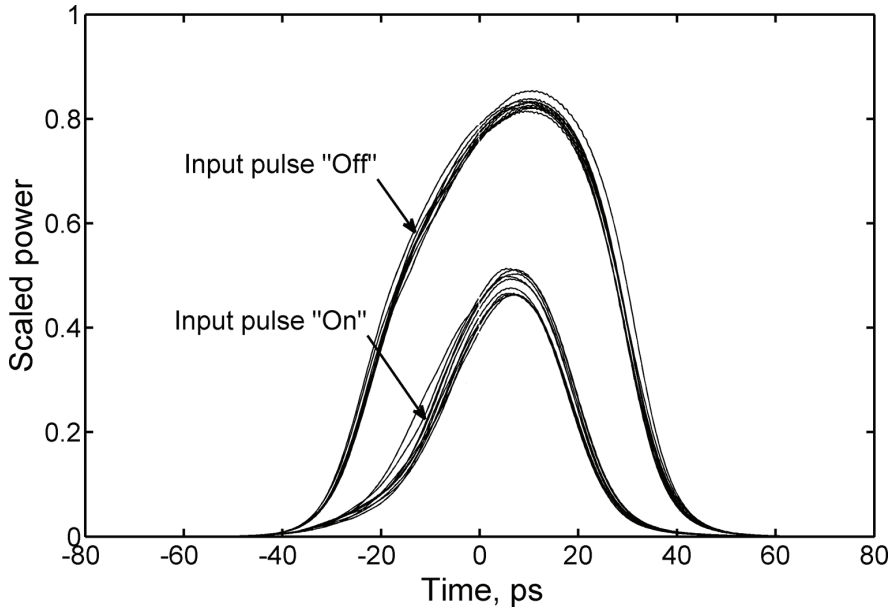

Figure 7. Output Stokes pulses for input pulses "ON" and "OFF."

From the above results, we can say that the setup of Raman circuit allows effective optical switching, logic operation, and noise reduction with signal of low power of the pump power. As we show above, to improve the operation of the Raman circuit we proposed the connection in series of fibers with normal and anomalous dispersion. We must consider that the power required for strong Raman amplification is lower than that required for the effects of MI and

http://dx.doi.org/10.5772/66320

pulse breakup in fibers with anomalous GVD [19]. The pulse breakup will affect the depletion of the pump pulse and amplification of the Stokes pulses. There are few works that are related to this problem, especially related to supercontinuum generation and Raman amplification [20].

3. Experimental results

Figure 8 shows the experimental setup, the setup used as a source of pump pulse is a diode laser with $\lambda = 1528$ nm. This diode laser is directly modulated by the pulse generator to generate pulses with duration of 2 ns. The pulses from the diode laser are amplified by an Erbium Doped Fiber Amplifier (EDFA) for power of several tens of Watts [21]. The pump pulses are introduced to the Coupler 1 (85/15), whose 85% port is spliced with the first stage comprising Fiber 1 + Fiber 2. In Fiber 1 we used the Corning SMF-28 fiber with anomalous GVD equal to 20 ps/nm-km, in the Fiber 2 we used the Corning SMF-LS dispersion shifted fiber with GVD equal to −6 ps/nm-km (normal dispersion at pump wavelength). The CW radiation with wavelength equal to 1620 nm is also introduced using the coupler 3 for two stages, the signal power introduced into Fiber 1 was 0.5 mW. The polarization controller inserted after the EDFA allows adjusting the polarization of the pump to provide maximum Raman amplification in the fibers because Raman amplification depends on polarization states of the pump and Stokes [22, 23]. The SRS in the first stage causes the signal amplification of 1620 nm and depletion pump pulse. In the experiment, two filters were used to reject the 1620 nm radiation at the end of the first stage. The Fabry-Perot (FP) filter and a broadband filter were used. For the launch the 1528 nm pump pulses and 1620 nm CW signal to the second stage of the experimental setup was used, Coupler 2 (90/10). The signal power of 1620 nm launched into fiber 3 was of 0.5 mW. We used 4.5 km of OFS True Wave (RS) fiber as fiber 3. With this configuration, we can measure simultaneously the pump pulse at the input of the first stage (pump monitoring, output 1), the pump output of the first stage (output 3), and pulses Stokes at the output of the second stage (output 2). We use the laser at this wavelength because it was what was available, but as the displacement of the wavelength between the signal and pumping must be very close to the maximum gain Raman (about 110 nm for the band of 1550 nm), thought we could use other lasers of around 1550 nm and can get a good operation of the device.

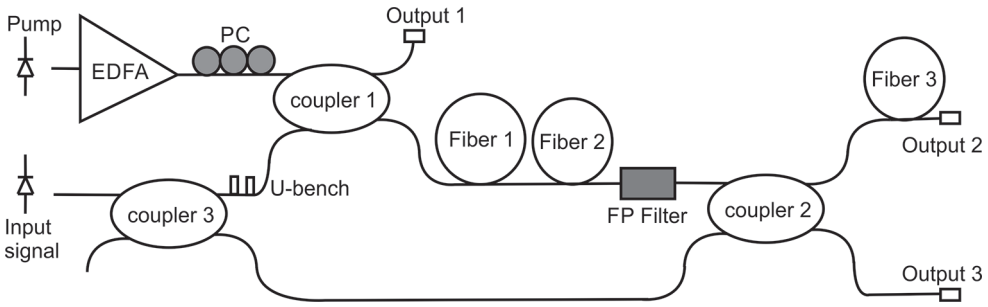

Figure 8. Experimental setup of Raman circuit.

To measure the Raman gains were launched to test fibers 0.5 mW of power with CW diode at 1620 nm. Stokes signal at output 3 of **Figure 8** was measured with a monochromator. The fiber used was SMF-28 with 100, 200, 300, 600, and 4500 m of length. The polarization of the pump was adjusted with the PC for maximum Raman amplification. The dependencies of powers Stokes with pump powers fit well with an exponential dependence, which corresponds to the Raman amplification given by exp (gP_bL/A_{eff}), where g is the coefficient of Raman amplification, P_b is the pumping power, A_{eff} is the effective area of the fiber core, and L is fiber length. In the results are also shown the critical power for breaking pulses. From these results we can say that the breaking of the pulse always starts with lower power compared to the Raman effect threshold. This can affect the efficiency of the switch since the breakup of the pulse starts before Raman amplification reaches significant values. The Raman gain average experimental value = 0.72 W^{-1}/km and the theoretical value for linearly polarized pump and Stokes = 0.72 W^{-1}/km (see **Figure 9**). Theoretical calculations agree well with the experiment.

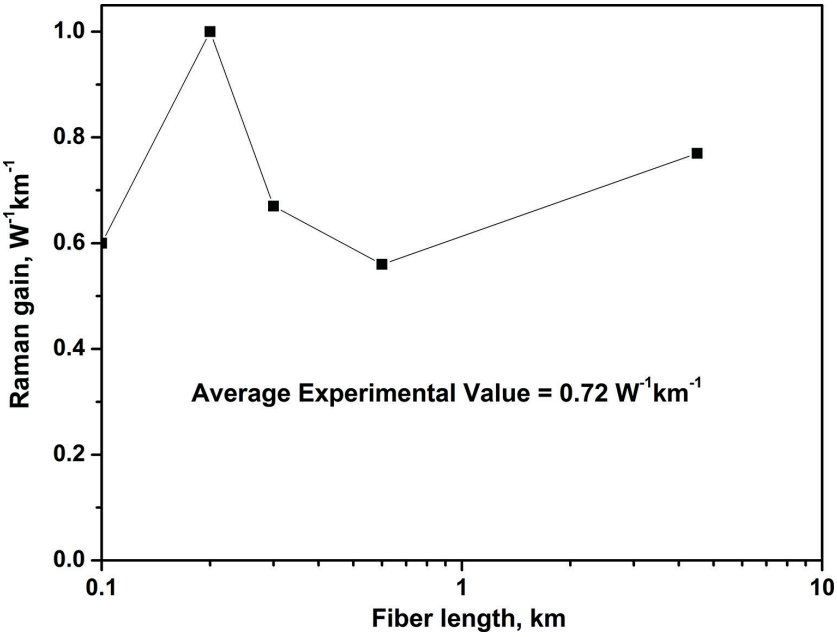

Figure 9. Raman gain.

The experimental setup is shown in **Figure 8**. We used the composed fiber, which consists of different spans of fiber 1 and fiber 2 for the investigated pump saturation in the first stage. **Figure 10** presents the results of waveforms of pump pulses at the output of the filter for different pump powers when only fiber 1 was used in the first stage. In the experiment, we used different span of fiber SMF-28. **Figure 10(a)** was obtained with a fiber length of 300 m and the inset is for the fiber with a length of 600 m. Strong depletion of the pump pulse was observed for the 300 m y 600 m of fiber even if the 1620 nm radiation was not applied. In this case, the effect of

http://dx.doi.org/10.5772/66320

the 1620 nm radiation on the pulse depletion was not detected. The maximum power at the FP filter output was measured to be equal to 7 W for 300 m y 3 w for 600 m. The pump depletion is caused by the pulse breakup process followed by the soliton self-frequency shift that results in broadening of the spectrum and the decrease of the power at the output of the FP filter.

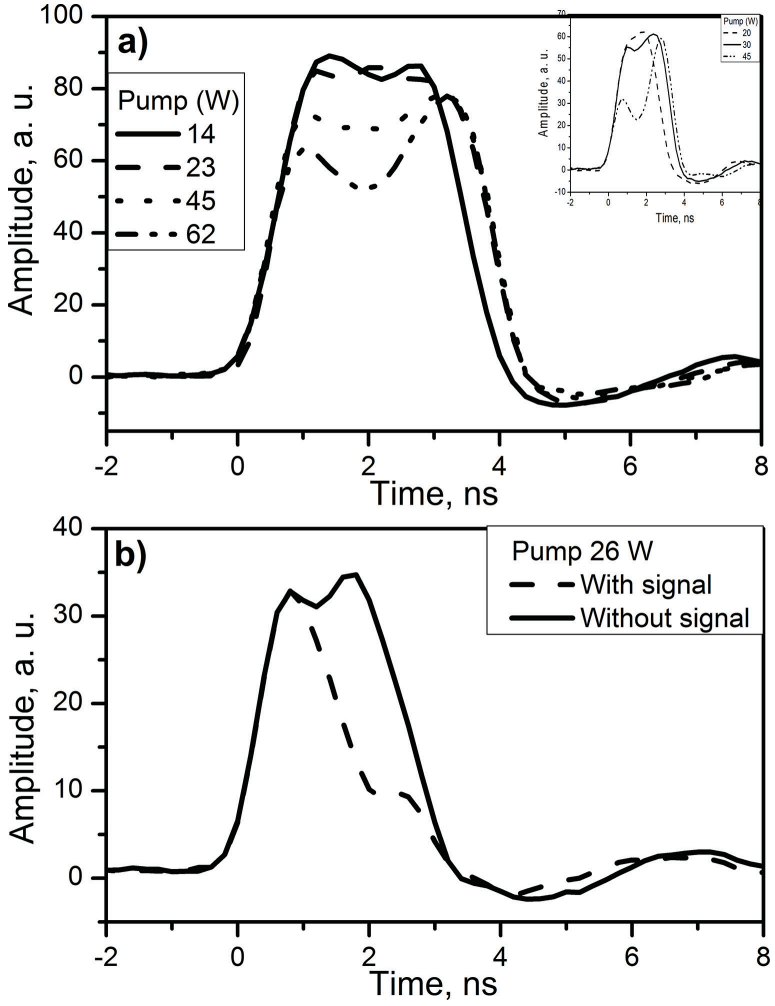

Figure 10. Pump pulses at the output of the FP filter when the SMF-28 fiber was used as the Fiber 1; (a) fiber length is equal to 300 m and the inset 600 m; (b) fiber length is equal to 1 km.

According to previous results, it can be concluded that for fiber lengths long critical power required for breaking pulses decays slower compared to the power required for Raman amplification. Therefore we assume that the effect of input radiation 1620 nm may be larger for larger fiber lengths. The pump saturation for 1 km of fiber SMF-28 is shown in **Figure 10(b)**,

the dashed line shows the pulse when radiation 1620 nm is off, and the solid line shows when we have 0.5 mW of 1620 nm radiation. The delay between pump pulses of 1528 nm and Stokes pulse 1620 nm for SMF-28 fiber is 2 ns for 1 km fiber, for this reason only the second half of the pulse is reduced. Depletion of the pump pulse when there was no input signal revealed that an effect of breaking pulse appears. The pump power for **Figure 10(b)** is 26 W.

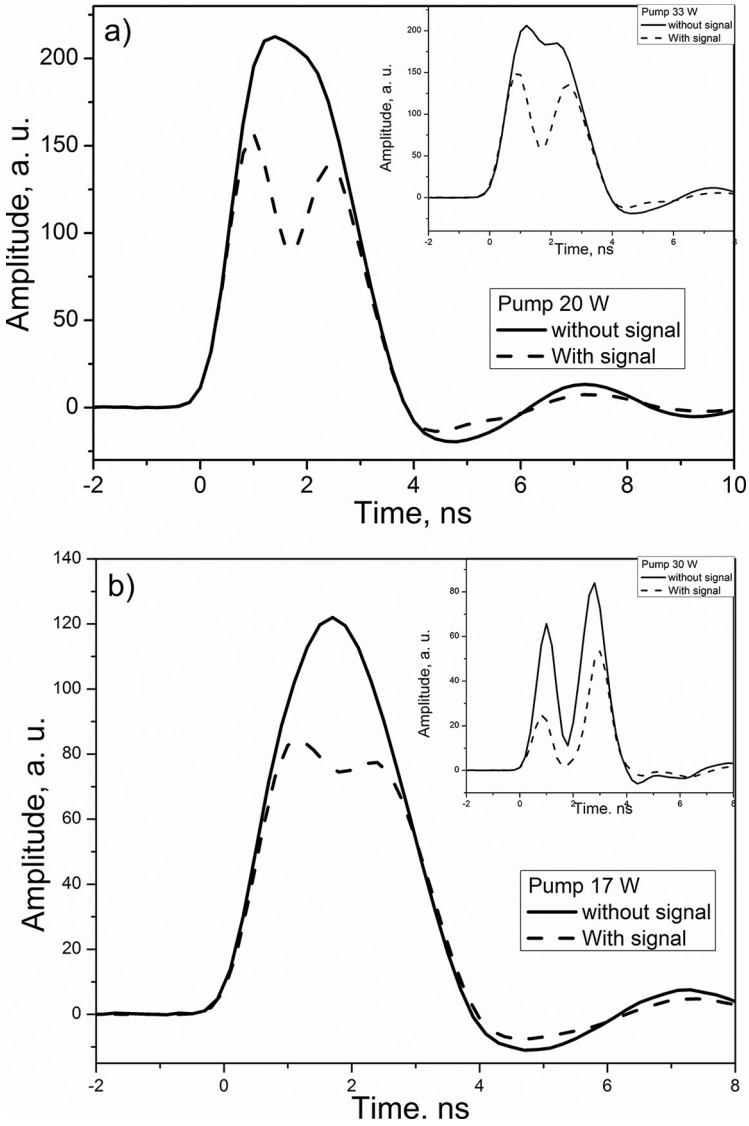

Figure 11. (a) Saturation of the pump by the input signal with 350 m of SMF-LS fiber for 20 W and the inset for 33 W pump power and (b) for 550 m SMF-Ls for 17 W and the inset for 30 W pump power.

http://dx.doi.org/10.5772/66320

Also tested in the experiment is the SMF-LS fiber, this fiber has normal dispersion for a wavelength of 1528 nm and so the effect of MI and breaking pulses are suppressed. The fiber shows conventional saturation of the pump and corroborates well with the simulations based on Eq. (1). **Figure 11** presents the results for a fiber of 350 and 550 m of length. **Figure 11(a)** shows pump power equal to 20 W and the inset of 33 W for 350 m of SMF-LS; **Figure 11(b)** shows pump power equal to 17 W and the inset of 30 W for 550 m of SMF-LS. Without input signal (solid line), no change in the waveform of the pump pulse is observed for **Figure 11(a)** and **(b)**. However, at 0.5 mW strong depletion of signal input power (dashed line) can be seen in **Figure 11(a)** and **(b)**. At 33 W for 350 m of SMF-LS and 30 W for 550 m of SMF-LS pumps power the depletion (solid line) is observed even without input signal, see insets of **Figure 11**.

We use a special fiber, consisting of a span of SMF-LS fiber spliced with another span of SMF-28 fiber, which was also tested in the experiment. Several tests were done and found that if the span of the fiber SMF-28 was respectively shorter than approximately 300 m, the effect of this span of fiber in low powers was negligible and depletion of the pump was determined by the fiber SMF-LS. For the case when we used 600 m of SMF-28 fiber spliced with 550 m fiber SMF-LS the effect of SMF-28 fiber was significant (with pump powers of 18 and 23 W). From these results, we can conclude that the effect of saturation of the pump by input signal was observed if the length of SMF-LS fiber is at least two times longer than the length of the SMF-28 fiber. For this case, the power required for MI effect is higher than that required for effective pump depletion. **Figure 12** presents an example of the output pump pulses for the first stage and the composed fiber consisted of a 550 m span of SMF-LS spliced with 300 m span of SMF-28, with pump power of 17 W and the inset for 20 W [17].

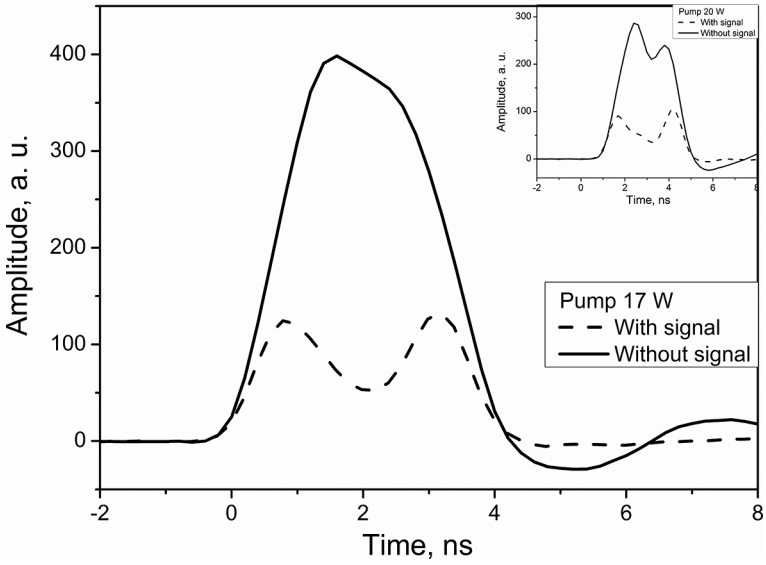

Figure 12. Saturation of the pump by the input signal if the first stage comprises a 550 m SMF-LS fiber connected to a 300 m SMF-28; pump power is 17 W and the inset for 20 W.

We can say that using the broadband filter obtain a considerable improvement in pump saturation, and with this result, we obtain a considerable improvement to the efficiency of the switch. The saturation measured for the composed fibers, which consists of a span of SMF-28 fiber spliced with another span of SMF-LS fiber, is shown in **Figure 13** and it presents the results of saturation for these fibers. **Figure 13(a)** presents results for 350 m SMF-LS fiber spliced with 300 m SMF-28 fiber, and **Figure 13(b)** presents results for 350 m SMF-LS fiber spliced with 600 m SMF-28 fiber. These graphs were obtained when using the broadband filter and spectral filter. We can see that when connecting the SMF-LS fiber, SMF-28 fiber can increase the saturation of the pump.

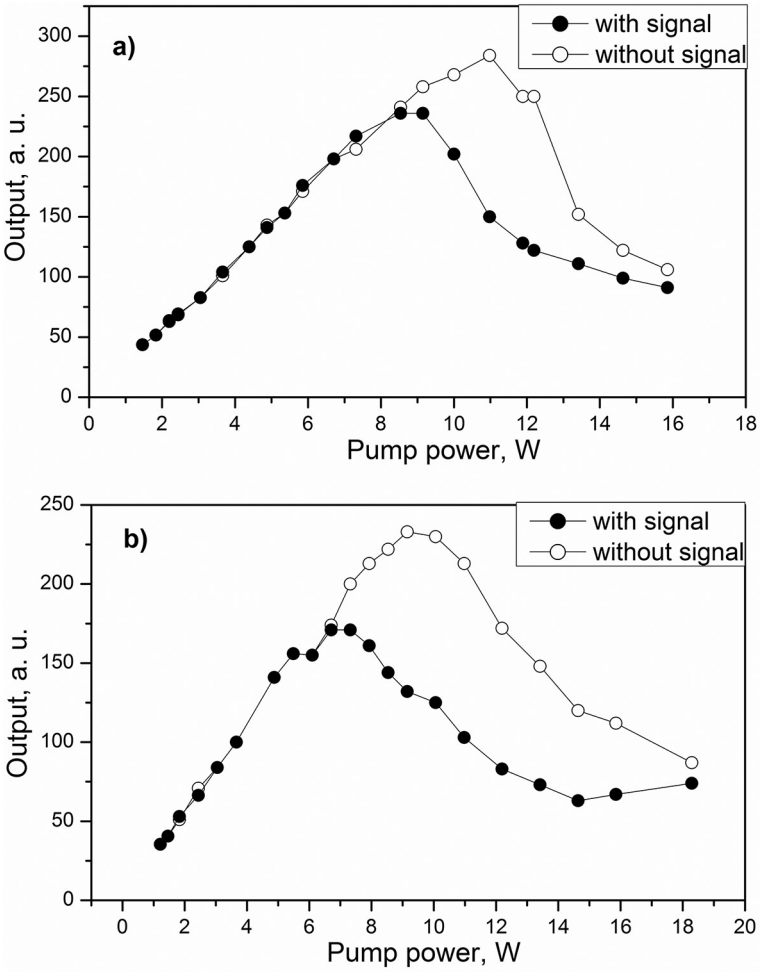

Figure 13. Saturation of peak power pump for variety of pump powers for two configurations: (a) 350 m SMF-LS fiber + 350 m SMF-28 fiber and (b) 350 m SMF-LS + 600 m SMF-28.

http://dx.doi.org/10.5772/66320

If the pump depletion in the first state of the SMF-28 fiber is determined by the MI, the depletion has to be dependent on the bandwidth of the filter inserted between the first and second stage. To show this, we use a broadband filter which is made with a spam of SMF-28 fiber. The difference between losses is sufficient to measure the depletion of pump of the broadband filter. **Figure 14** shows the results of the depletion measured with the broadband filter and the inset shows the results of the depletion measured with Fabry-Perot filter. We can see from the figure that with the narrow band filter pump depletion occurs in low power pump (about 5 W) and for the case with the broadband filter pump depletion occurs in about 30 W of pump power. We can conclude that the problem connected with the MI could be overcome using wideband filter between the first and the second stage. We can consider, for example, a filter based on a liquid filled photonic crystal fiber filter [24].

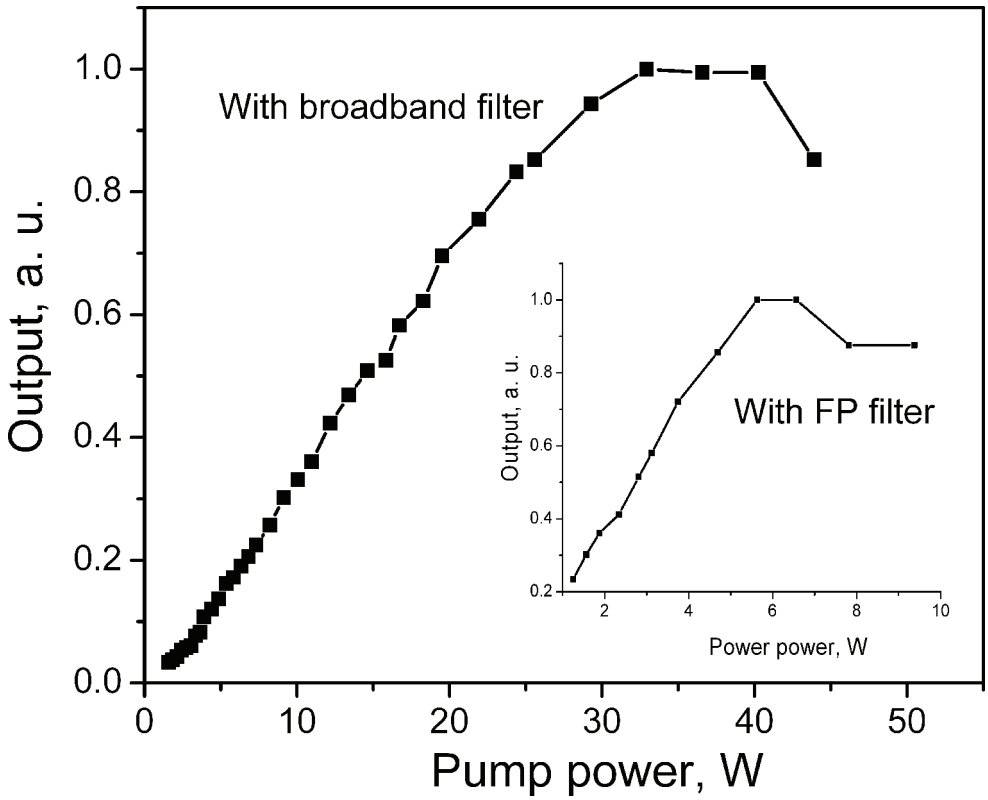

Figure 14. Saturation of pump measured with broadband and narrowband filter.

We investigate the experimental setup of the Raman circuit composed of two stages. In stage 1, we used different combinations of the SMF-LS fiber and SMF-28 fiber, and for stage 2, we used OFS True Wave (RS) fiber with 4.5 km of length. The results show the waveforms of the signal

pulses at the output 2 of the experimental setup. We used for stage 1: SMF-LS with different length; the composed fibers, which consists of a span of SMF-LS fiber spliced with another span of SMF-28 fiber. The results of **Figure 15(a)** were obtained with 350 m of SMF-LS as the first stage at 37 W pump power and the inset is for 550 m of SMF-LS at 23 W; the results of **Figure 15(b)** were obtained with 550 m of SMF-LS spliced with 600 m of SMF-28 used as the first stage at 18 W pump power. The inset of **Figure 15(b)** show magnifications of the output signal when input signal is applied.

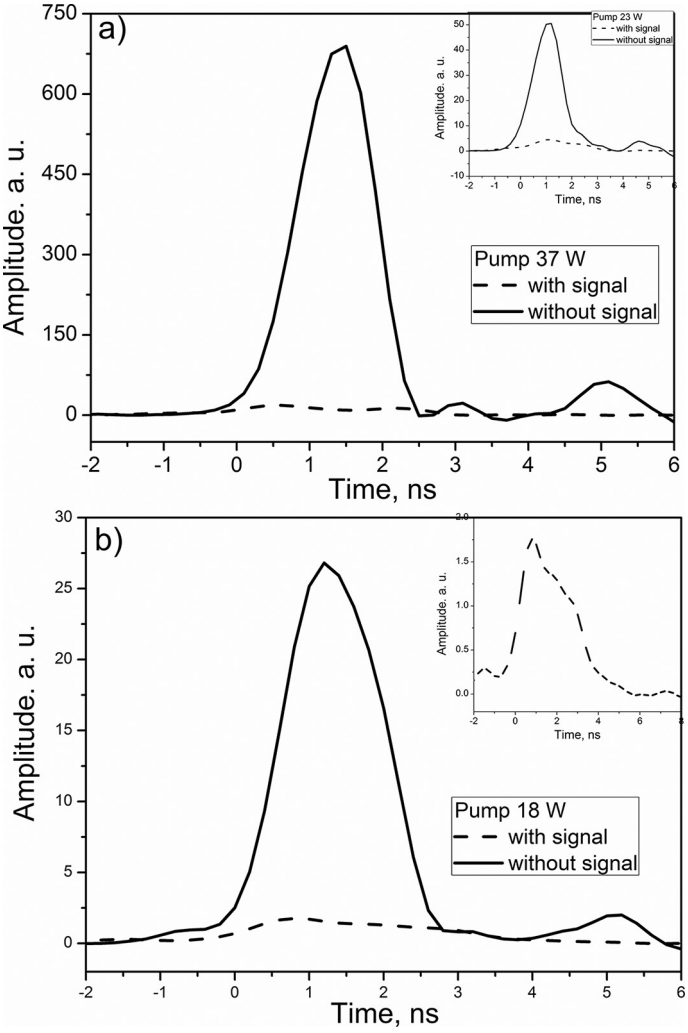

Figure 15. The waveforms of the output signal at 1620 nm at the output 2 of the experimental setup; dashed line with input signal (OFF), solid line without input signal (ON). The first stage consists of the 350 m of the SMF-LS fiber and the inset for 550 m of SMF-LS fiber (a); the first stage consists or of the 350 m SMF-LS connected to the 600 m SMF-28 the inset show the magnification of the when input signal is applied (b).

http://dx.doi.org/10.5772/66320

Finally, we measured the ratio of output energy without input signal ("OFF") and with input signal ("ON") for different pump powers. **Figure 16** shows the dependencies of the contrast on the pump power. The dependencies are shown for the first stage consisting of the 350 m SMF-LS fiber, **Figure 16(a)**, and for the first stage consisting of the 350-m SMF-LS and the 600 m SMF-28 fiber, **Figure 16(b)**. We can see that the best results from our configuration are for 350 m from the SMF-LS fiber in the first stage. For this configuration, the contrast OFF/ON came up to 27. With 500 m of SMF-LS in the first stage maximum contrast was equal to 7 and for configuration of 600 m of SMF-28 m spliced with 500 m of SMF-LS increase the contrast to 13.

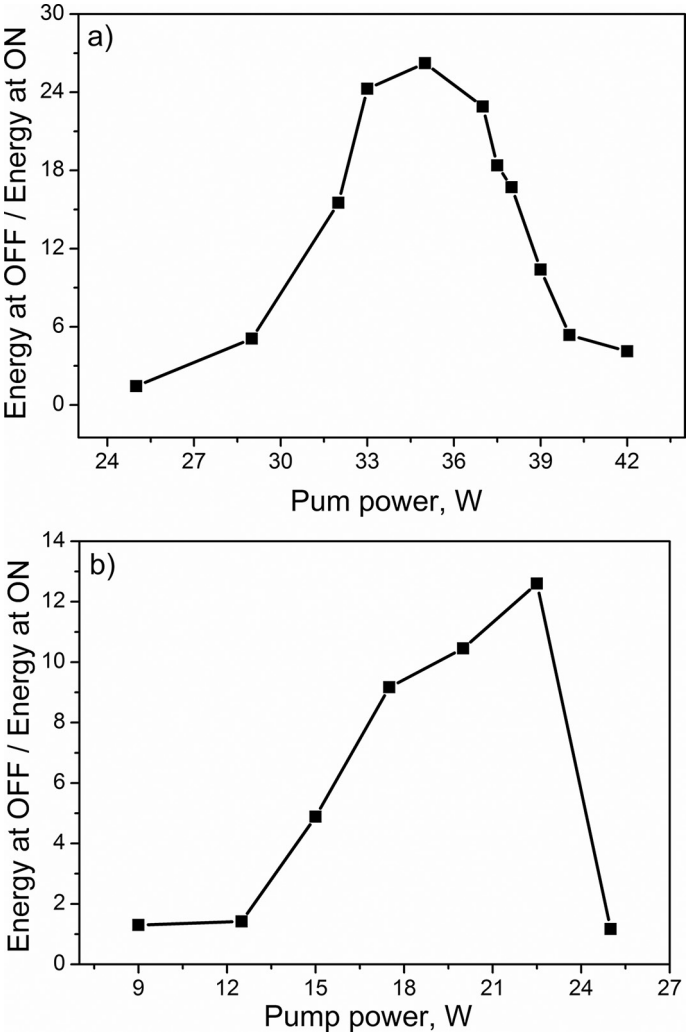

Figure 16. Energy of Stokes pulses, (a) for 350 m SMF-LS in the first stage; (b) for 550 m SMF-LS + 600 m SMF-28 in the first stage.

4. Conclusions

We investigate experimentally and theoretically an all-optical switch based on the SRS and demonstrate its viability. The use of SRS to design an all-optical switch circuit makes it possible to use very low powers of signal to control respectively strong pulses. The best contrast (the ratio of signal energy at the output when the input signal is ON/OFF) was 15 dB in pump peak power of 6 W and input signal only of 0.5 mW. Since there is a big difference between the wavelengths of pumping and signal, the walk-off between pump and Stokes is inevitable. We investigate the possibility to avoid degradation of circuit operation by the walk-off effect connecting fibers with normal and anomalous dispersion. We found that fibers with anomalous GVD effect of the MI and the breaking pulse appear lower than those required for a strong Raman amplification powers. We propose to use the spectral filter large bandwidth between states of Raman circuit for reducing problems of breaking pulses. We have built a simple configuration of the device with efficient switching and low power pump. Therefore, the experimental setup is compact and can be carried to another laboratory, and results are repeatable, i.e., the measurements are not dependent on environmental parameters.

Acknowledgements

The authors thank the Mexican Council for Science and Technology (CONACyT) for providing financial support for the realization of this project and the Proyecto PROMEP (Profocie) DSA/103.5/15/7129.

Author details

Ariel Flores-Rosas[1]*, Evgeny A. Kuzin[2], Orlando Díaz-Hernández[1], Gerardo J. Escalera-Santos[1], Roberto Arceo-Reyes[1], Baldemar Ibarra-Escamilla[2] and Víctor I. Ruiz-Pérez[3]

*Address all correspondence to: ariel.flores@unach.mx

1 Facultad de Ciencias en Física y Matemáticas, Universidad Autónoma de Chiapas, Tuxtla Gutiérrez, Chiapas, México

2 Departamento de Óptica, Instituto Nacional de Astrofísica, Óptica y Electrónica (INAOE), Puebla, México

3 Instituto Tecnológico de Culiacán, Culiacán, Sinaloa, México

References

[1] N. Nishizawa and Y. Ukai. Ultrafast all optical switching using pulse trapping in birefringent fibers. Optics Express. 2005;**13**(20):8128–8135. DOI: 10.1364/OPEX.13.008128

[2] M. Bajcsy, S. Hofferberth, V. Balic, T. Peyronel, M. Hafezi, A.S. Zibrov, V. Vuletic, and M.D. Lukin. Efficient all-optical switching using slow light within a hollow fiber. Physical Review Letters. 2009;**102**(20):203902. DOI: http://dx.doi.org/10.1103/PhysRevLett.102.203902

[3] N. J. Doran and David Wood. Nonlinear-optical loop mirror. Optics Letters. 1988;**13**(1):56–58. DOI: 10.1364/OL.13.000056

[4] B.E. Olsson and D.J. Blumenthal. All-optical demultiplexing using fiber cross-phase modulation (XPM) and optical filtering. IEEE Photonics Technology Letters. 2001;**13**(8):875–877. DOI: 10.1109/68.935833

[5] E. Ciaramella and T. Stefano. All-optical signal reshaping via four-wave mixing in optical fibers. IEEE Photonics Technology Letters. 2000;**12**(7):849–851. DOI: 10.1109/68.853523

[6] T. Fujisawa and M. Koshiba. All-optical logic gates based on nonlinear slot-waveguide couplers. Journal of the Optical Society of America B. 2006;**23**(4):684–691. DOI: 10.1364/JOSAB.23.000684

[7] R. Dekker, A. Driessen, T. Wahlbrink, C. Moormann, J. Niehusmann, and M. Först. Ultrafast Kerr-induced all-optical wavelength conversion in silicon waveguides using 1.55 μm femtosecond pulses. Optics Express. 2006;**14**(18):8336–8346. DOI: 10.1364/OE.14.008336

[8] M.N. Islam, C.E. Soccolich, and D.A.B. Miller. Low-energy ultrafast fiber soliton logic gates. Optics Letters. 1990;**15**(16):909–911. DOI: 10.1364/OL.15.000909

[9] A.I. Siahlo, L.K. Oxenløwe, K.S. Berg, A.T. Clausen, P.A. Andersen, C. Peucheret, A. Tersigni, P. Jeppesen, K.P. Hansen, and J.R. Folkenberg. A high-speed demultiplexer based on a nonlinear. IEEE Photonics Technology Letters. 2003;**15**(8):1147–1149. DOI: http://orbit.dtu.dk/fedora/objects/orbit:18529/datastreams/file_4226957/content.

[10] B. Ibarra-Escamilla, E.A. Kuzin, D.E. Gomez-Garcia, F. Gutierrez-Zainos, S. Mendoza-Vasquez, and J.W. Haus. A mode-locked fibre laser using a Sagnac interferometer and nonlinear polarization rotation. Journal of Optics A: Pure and Applied Optics. 2003;**5**(5):S225. DOI: http://dx.doi.org/10.1088/1464-4258/5/5/370

[11] E. Ciaramella, F. Curti, and S. Trillo. All-optical signal reshaping by means of four-wave mixing in optical fibers. IEEE Photonics Technology Letters. 2001;**13**(2):142–144. DOI: 10.1109/68.910515

[12] S. Yamashita and S. Mazumder. Optical 2R regeneration using cascaded fiber four-wave mixing with suppressed spectral spread. IEEE Photonics Technology Letters. 2006;**18**(9):1064–1066. DOI: 10.1109/LPT.2006.873475

[13] C. Headley and G. P. Agrawal. Raman Amplification in Fiber Optical Communication. 1st ed. San Diego, CA, USA: Elsevier Academic Press; 2005. 152 p. DOI: 012044506-9

[14] A. Uchida, M. Takeoka, T. Nakata, and F. Kannari. Wide-range all-optical wavelength conversion using dual-wavelength-pumped fiber Raman converter. Journal of Lightwave Technology. 1998;**16**(1):92–99. DOI: 10.1109/50.654989

[15] F. Ahmed and N. Kishi. All-fiber wavelength conversion of ultra-fast signal with enhanced extinction ratio using stimulated Raman scattering. Optical Review. 2003;**10**(1):43–46. DOI: 10.1007/s10043-003-0043-6

[16] V.I. Belotitskii, E.A. Kuzin, M.P. Petrov, and V.V. Spirin. Demonstration of over 100 million round trips in recirculating fibre loop with all-optical regeneration. Electronics Letters. 1993;**29**(1):49–50. DOI: 0013-5194

[17] A. Flores-Rosas, E.A. Kuzin, O. Pottiez, B. Ibarra-Escamilla, and M. Duran-Sánchez. Optical switch based on stimulated Raman scattering. Optical Engineering. 2011;**50**(7):071101-7. DOI: 10.1117/1.3558851

[18] A. Flores-Rosas, E.A. Kuzin, B. Ibarra-Escamilla, O. Pottiez, and M. Duran-Sánchez. The on-off contrast in an all optical switch based on stimulated Raman scattering in optical fibers. In: Benjamin J. Eggleton; Alexander L. Gaeta; Neil G. R. Broderick, editors. Nonlinear Optics and Applications IV; June 04, 2010; Brussels, Belgium. Bellingham, USA: Spie Digital Library; 2010. p. 7728. DOI: 10.1117/12.854737

[19] G. P Agrawal. Nonlinear Fiber Optics. 1st ed. San Diego, CA, USA: Academic Press; 2001. 442 p. DOI: 012045144-1

[20] A. E. El-Taher, J. D. Ania-Castañon, V. Karalekas, and P. Harper. High efficiency supercontinuum generation using ultra-long Raman fiber cavities. Optics Express. 2009;**17**(20):17909–17915. DOI: 10.1364/OE.17.017909

[21] M. Bello-Jimenez, E. A. Kuzin, B. Ibarra-Escamilla, and A. Flores-Rosas. Optimization of the two-stage single-pump erbium-doped fiber amplifier with high amplification for low frequency nanoscale pulses. Optical Engineering. 2007;**46**(12):125007. DOI: 10.1117/1.2823495

[22] Q. Lin and G.P. Agrawal. Vector theory of stimulated Raman scattering and its application to fiber-based Raman amplifiers. Journal of the Optical Society of America B. 2003;**20**(8):1616–1631. DOI: 10.1364/JOSAB.20.001616

[23] S. Sergeyev, S. Popov, and A.T. Friberg. Modeling polarization-dependent gain in fiber Raman amplifiers with randomly varying birefringence. Optics Communications. 2006;**262**(1):114–119. DOI: 10.1016/j.optcom.2005.12.045

[24] S. Torres-Peiró, A. Díez, J.L. Cruz, and M.V. Andrés. Fundamental-mode cutoff in liquid-filled Y-shaped microstructured fibers with Ge-doped core. Optics Letters. 2008;**33**(22):2578–2580. DOI: 10.1364/OL.33.002578